FRENCH, S. & WILSON, K. (1978). *Acta Cryst.* A**34**, 517–525.
GOPAL, R., RUTHERFORD, J. S. & ROBERTSON, B. E. (1980). *J. Solid State Chem.* **32**, 29–40.
HALL, S. R. & STEWART, J. M. (1989). Editors. *XTAL2.6 User's Manual.* Univs. of Western Australia, Australia, and Maryland, USA.
HAWTHORNE, F. C. (1986). *Am. Mineral.* **71**, 206–209.
HENSEN, B. J. (1977). *Phys. Earth Planet. Inter.* **14**, P3–P5.
HYDE, B. G., WHITE, T. J., O'KEEFFE, M. & JOHNSON, A. W. S. (1982). *Z. Kristallogr.* **160**, 53–62.
JOUBERT, J. C. & DURIF, A. (1964). *Bull. Soc. Fr. Mineral. Cristallogr.* **87**, 47–49.
KRISHNAMACHARI, N. (1970). PhD Thesis, Department of Chemistry, McMaster Univ., Canada.
KRISHNAMACHARI, N. & CALVO, C. (1970*a*). *Can. J. Chem.* **48**, 3124–3131.
KRISHNAMACHARI, N. & CALVO, C. (1970*b*). *Can. J. Chem.* **48**, 881–889.
KRISHNAMACHARI, N. & CALVO, C. (1971). *Can. J. Chem.* **49**, 1629–1637.
KRISHNAMACHARI, N. & CALVO, C. (1973). *Acta Cryst.* B**29**, 2611–2613.
KRISHNAMACHARI, N. & CALVO, C. (1974). *Can. J. Chem.* **52**, 46–50.
MOORE, P. B. (1972). *Am. Mineral.* **57**, 24–35.
OZOG, J., KRISHNAMACHARI, N. & CALVO, C. (1970). *Can. J. Chem.* **48**, 388–389.
PALAZZI, M. & GUÉRIN, H. (1978). *Bull. Soc. Chim. Fr.* pp. I119–I120.
POULSEN, S. J. & CALVO, C. (1968). *Can. J. Chem.* **46**, 917–927.
SAUERBREI, E. E., FAGGIANI, R. & CALVO, C. (1973). *Acta Cryst.* B**29**, 2304–2306.
SHANNON, R. D. & CALVO, C. (1972). *Can. J. Chem.* **50**, 3944–3949.
TAYLOR, J. B. & HEYDING, R. D. (1958). *Can. J. Chem.* **36**, 597–606.

Acta Cryst. (1991). B**47**, 462–468

Structural and Thermal Parameters for Rutile and Anatase

BY C. J. HOWARD

Australian Nuclear Science and Technology Organisation, Lucas Heights Research Laboratories, Private Mail Bag 1, *Menai, New South Wales* 2234, *Australia*

AND T. M. SABINE AND FIONA DICKSON*

University of Technology, Sydney, PO Box 124, *Broadway, New South Wales* 2007, *Australia*

(*Received* 6 *September* 1990; *accepted* 12 *March* 1991)

Abstract

Neutron powder diffraction patterns from rutile (TiO_2, $P4_2/mnm$, $a = 4{\cdot}594$, $c = 2{\cdot}959$ Å) and anatase (TiO_2, $I4_1/amd$, $a = 3{\cdot}785$, $c = 9{\cdot}514$ Å) have been analysed by the Rietveld method. The positional parameters were determined to be $x_O = y_O = 0{\cdot}30478$ (6) in rutile and $z_O = 0{\cdot}20806$ (5) in anatase. The anisotropic thermal parameters were also determined. The results from this constant-wavelength neutron diffraction study are in remarkably good agreement with the results from a recently published analysis of time-of-flight neutron data from the same phases. A comparison is made with results from earlier X-ray single-crystal investigations of these polymorphs of titania, and again the agreement is good. In particular, there is no evidence for any significant difference between X-ray and neutron determinations of the oxygen position such as might have resulted from polarization effects. The thermal vibrations show marked anisotropy, which appears to be determined by the stereochemistry of the crystal structure. The Debye temperatures estimated from the diffraction data are 600 (10) K for rutile and 520 (10) K for anatase at room temperature.

1. Introduction

The crystal structures of rutile and anatase, two of the polymorphs of titanium dioxide, were first described by Vegard (1916). The structures have been redetermined from time to time, using improved techniques to obtain more accurate crystal structure data. These additional investigations have been motivated by interests in the electronic properties, the nature of the bonding, and the general relationship between electronic properties and crystal structure in these materials. The further work includes an X-ray powder diffraction study of anatase and rutile (Cromer & Herrington, 1955), single-crystal X-ray diffraction investigations of anatase (Horn, Schwerdtfeger & Meagher, 1972) and of rutile (Abrahams & Bernstein, 1971; Shintani, Sato & Saito, 1975; Gonschorek, 1982), and neutron diffraction investigations of rutile using both single-crystal (Gonschorek & Feld, 1982) and powder (Sabine & Howard, 1982) techniques. For rutile,

* Present address: Bristows Cooke and Carpmael, 10 Lincoln's Inn Fields, London WC2A 3BP, England.

0108-7681/91/040462-07$03.00 © 1991 International Union of Crystallography

which has received rather more attention than the other polymorphs, neutron scattering methods have been employed to determine the phonon dispersion curves, and a shell model which includes first- and second-neighbour forces has been developed to fit the results (Traylor, Smith, Nicklow & Wilkinson, 1971). The most recent contribution has been a redetermination, by Rietveld analysis of time-of-flight (TOF) neutron powder diffraction data, of the crystal structures of both anatase and rutile at 15 and 295 K (Burdett, Hughbanks, Miller, Richardson & Smith, 1987).

The number of accurate crystal structure determinations now is such that it has become worthwhile to make detailed comparisons of the results obtained using different techniques. In this paper we report a new (*cf.* Sabine & Howard, 1982) higher statistics and shorter wavelength neutron powder diffraction measurement on rutile, and a corresponding measurement on anatase. The measurements were made at room temperature. The diffraction patterns have been analysed by the Rietveld (1969) method. In each case the one variable positional parameter and appropriate anisotropic thermal parameters have been refined. The results are found to be in remarkably good agreement with those from the TOF study mentioned above (Burdett *et al.*, 1987). The results are also compared with the results from a number of the earlier investigations by X-ray and neutron methods. This comparison confirms that there is no significant difference between the positional parameters determined by X-ray diffraction and those determined using neutrons. Finally, it is shown that the anisotropy seen in the thermal vibration parameters correlates strongly with the stereochemistry in the crystal structure.

2. Experimental

The anatase powder was analytical reagent grade powder from British Drug Houses Chemicals. Scanning electron microscopy (SEM) showed that the particle size in this powder was of the order of 0·1–0·2 μm. The powder was lightly ground with a pestle and mortar to break up aggregates, and about 9·5 g of the powder was loaded into a standard 16 mm diameter by 50 mm high vanadium sample can for the measurement.

The rutile sample was a 14 mm diameter sintered cylinder, from the same batch as the sample used in our previous study (Sabine & Howard, 1982). It was prepared by pressing analytical reagent grade TiO_2 at room temperature, then sintering in air at 1573 K for 13 h. The sample was light-grey rather than white: such discolouration of sintered samples has been noted previously and attributed to a slight departure from stoichiometry, specifically an O/Ti atomic ratio of about 1·985 (Straumanis, Ejima & James, 1961). The diffraction pattern shows no evidence of impurity phases, and a test refinement from the diffraction pattern allowing for variation of the occupancy of the oxygen site gave a value of 1·995 (11) for the O/Ti ratio. The grain-size distribution was determined using SEM, with calibration of the magnification using a 2000 lines per inch electroformed mesh supplied by Polaron Instruments Inc. Fig. 1 displays a typical micrograph, and shows the grain-size distribution obtained. The peak in the distribution corresponds to a grain size of 12 μm.

The diffraction patterns were recorded using the eight-counter fixed-wavelength high-resolution powder diffractometer (HRPD) at the Australian Nuclear Science and Technology Organisation's

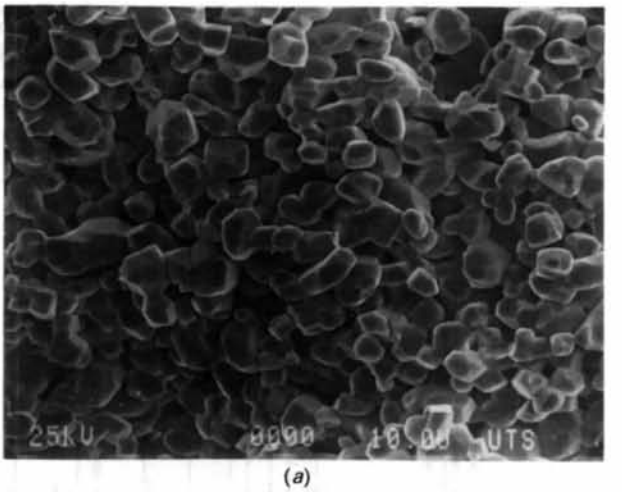

(*a*)

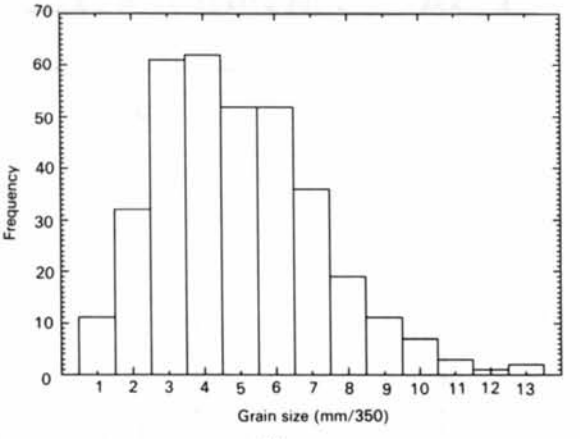

(*b*)

Fig. 1. Scanning electron microscopy of rutile. (*a*) A typical micrograph of material from the interior of the neutron diffraction sample, after that material had been exposed by fracture. The marker corresponds to 10 μm. (*b*) The grain-size distribution, obtained from several micrographs (at × 350 magnification) taken from different parts of the specimen. The peak in this distribution corresponds to a grain size of 12 μm.

research reactor HIFAR.* This instrument (in an earlier single-counter configuration) has been described by Howard, Ball, Davis & Elcombe (1983). Certain details of the data collection are given in Table 2. The patterns were recorded at room temperature, using neutrons of wavelength 1·377 Å. Counts at each step were recorded until counts in the incident beam monitor reached a preset value. The data for anatase were aggregated from two patterns recorded successively. The observed diffraction patterns, indicated by the crosses, can be seen in Fig. 2.

3. Data analysis and results

The basic crystallographic data, for rutile and anatase, are collected in Table 1. The neutron scattering lengths used were −3·438 and 5·805 fm for Ti and O respectively.

The Rietveld method structure and profile refinements were carried out using the program *LHPM*1 (Hill & Howard, 1986). The refinements incorporated weights based on the observed step intensities, and were continued until the shift in any parameter was less than one tenth of its estimated standard deviation (e.s.d.). Further pertinent details are shown in Table 2. The background was taken to be a quadratic function of 2θ, and was refined simultaneously with the unit-cell, zero-point, scale, peak width/shape/asymmetry and crystal structure parameters. Preferred orientation and extinction parameters were also refined. In Table 2, the count of 'structural' parameters includes the one positional parameter in each structure, the appropriate anisotropic thermal parameters and the cell parameters. The peak profile was Voigtian, with the widths of the Gaussian and Lorentzian components coded to vary in accordance with the Caglioti, Paoletti & Ricci (1958) function (to describe instrumental resolution,

* Lists of the observed step-scan neutron diffraction data for rutile and anatase have been deposited with the British Library Document Supply Centre as Supplementary Publication No. SUP 54035 (9 pp.). Copies may be obtained through The Technical Editor, International Union of Crystallography, 5 Abbey Square, Chester CH1 2HU, England.

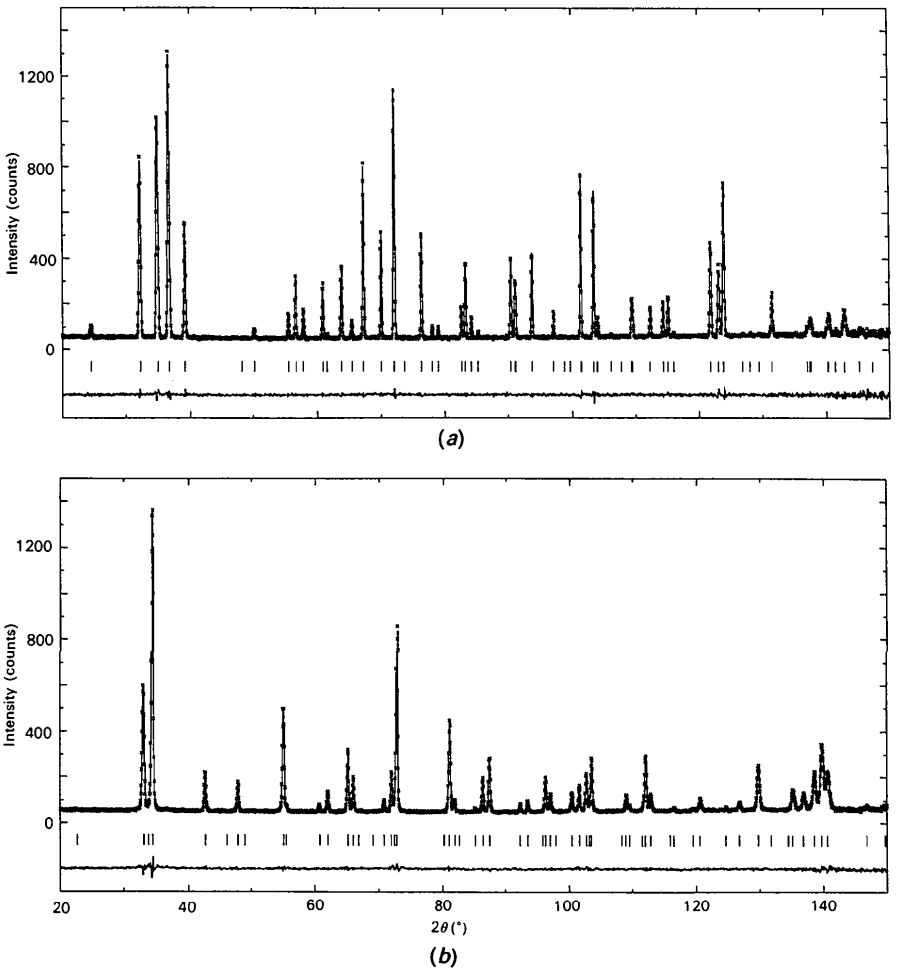

Fig. 2. Plot output showing the Rietveld method fits to the diffraction patterns from (*a*) rutile and (*b*) anatase. The observed data are indicated by crosses and the calculated pattern is the continuous line overlying them. The short vertical lines below the pattern mark the positions of all the Bragg reflections, and the lower curve is the difference between the observed and calculated patterns plotted on the same scale.

Table 1. *Basic crystallographic data for rutile and anatase*

	Rutile	Anatase
Formula	TiO_2	TiO_2
Space group	$P4_2/mnm$ (No. 136)	$I4_1/amd$ (No. 141)*
Lattice parameters†		
a (Å)	4·5937	3·7845
c (Å)	2·9587	9·5143
Ti Site	2(*a*)	4(*a*)
Position (x,y,z)	0,0,0	0,0,0
Constraints on thermal parameters‡	$U_{11} = U_{22}$ $U_{13} = U_{23} = 0$	$U_{11} = U_{22}$ $U_{12} = U_{13} = U_{23} = 0$
O Site	4(*f*)	8(*e*)
Position (x,y,z)	$u,u,0$	0,0,z
Constraints on thermal parameters‡	$U_{11} = U_{22}$ $U_{13} = U_{23} = 0$	$U_{12} = U_{13} = U_{23} = 0$

* For this space group we take the origin at $\bar{4}m2$ (origin choice 1).

† X-ray lattice parameters. They are, for rutile from Abrahams & Bernstein (1971), and for anatase from Rao, Naidu & Iyengar (1970).

‡ The temperature factor is taken to be $\exp[-2\pi^2(U_{11}h^2a^{*2} + \cdots + 2U_{23}klb^*c^*)]$. The constraints have been obtained by reference to the work of Peterse & Palm (1966).

Table 2. *Data collection and refinement details*

	Rutile	Anatase
Neutron wavelength (Å)	1·377	1·377
2θ scan range (°)	20–150	18–160
2θ scan step (°)	0·05	0·05
Max. step intensity*	10^4	2×10^4
No. of reflections	61	69
No. of parameters refined		
Total	21	20
Structural	9	8
Profile	5	5
Background	3	3
Other	4	4
Preferrred orientation parameter† (vector [001])	0·999 (2)‡	0·994 (3)
Crystallite size, from line broadening† (μm)	1·2 (2)	0·12 (1)
Mosaic block size (spherical), from extinction† (μm)	5 (1)	3 (2)
R_{wp} (%)§	4·54	4·30
R_{exp} (%)§	4·16	3·16
R_B (%)§	0·67	0·70

* Aggregate count in eight and sixteen detectors for rutile and anatase respectively.

† See text.

‡ The figures in parentheses here and elsewhere in the tables indicate the standard deviations (referred to the least significant digit) as estimated in the refinement.

§ Standard Rietveld method agreement index (Young, Prince & Sparks, 1982).

and the effects of possible crystallite strain) and with $\sec\theta$ (to describe crystallite size effects) respectively. From the widths of the Lorentzian components, a crystallite size parameter was derived (Hill & Howard, 1986). Instrumental peak asymmetry was modelled using a sum of five Voigtians, this sum being dependent on a single asymmetry parameter. The intensity in each peak was calculated out to two full-widths at half-maximum from the peak centre. Preferred orientation was described by the one-parameter March model (March, 1932; Dollase, 1986), taking [001] as the unique direction in each material. The value of the March preferred orientation parameter is 1·0 in the absence of preferred orientation, and less than or greater than 1·0 according to whether there is a preponderance or scarcity of the chosen vectors along the sample axis in the Debye–Scherrer geometry employed. Refined values of this parameter (Table 2) suggest very little preferred orientation in the samples under study.

The particle size in the anatase (in the range 0·1–0·2 μm) means that for this material extinction should be negligible. However, given the larger grain size for rutile, and the results of powder diffraction studies of magnesia (Sabine, 1985; Sabine, Von Dreele & Jorgensen, 1988) which showed extinction can be significant in powder work, extinction has been included in the calculations. The extinction model of Sabine (1988) was coded into the computer program, and the extinction parameter (*i.e.* the size of the mosaic block, assumed spherical) was refined during the analysis. The values for the mosaic block size (in Table 2) mean that, at the neutron wavelength used in this study, extinction effects should be small. This is confirmed by comparing results of refinements with and without extinction – in such a comparison we found that in no case did the two parameter values obtained differ by more than half of the estimated standard deviation.

Fig. 2 shows the fits between calculated and observed diffraction patterns obtained in the present work. The usual measures of fit are reported in Table 2. The results obtained for the positional parameter and the anisotropic thermal parameters, for rutile and for anatase, are shown as the left-hand entries in Tables 3 and 4 respectively. The results for a selection of the other parameters discussed above (preferred orientation, extinction, crystallite size) are included in Table 2.

4. Discussion

4.1. *Comparison with previous experimental results*

The results from previous accurate neutron and X-ray studies of rutile and anatase are recorded in Tables 3 and 4, alongside the results from the present work. As the results obtained in the different studies are generally in good agreement, detailed comparisons are worthwhile.

The first comparison of interest is that between the results from this work and those from Burdett *et al.* (1987). Both sets of results were obtained by Rietveld method refinement from neutron powder diffraction data, the data being recorded using a conventional diffractometer in one case (this work) and a time-of-flight diffractometer in the other. The values obtained for the atomic positional parameters, in rutile and anatase, are in extremely good agreement. The anisotropic thermal vibration parameters show differences of no more than three combined e.s.d.'s for rutile, but a little more in anatase. Very similar anisotropies are indicated for every atom except Ti in anatase, which was constrained to be isotropic in the

Table 3. *Atomic positional and anisotropic thermal parameters* ($Å^2 \times 10^3$) *for rutile at room temperature*

		Neutron determinations			Single-crystal X-ray determinations		
		Powder	Powder (TOF)	Single crystal			
		Present work	Burdett *et al.*	Gonschorek & Feld	Abrahams & Bernstein*	Shintani *et al.*	Gonschorek
Ti	U_{11}	6·8 (3)	5·5 (2)	6·9 (5)	6·4 (1)	6·99 (4)	6·68 (4)
	U_{12}	−0·4 (3)	−0·3 (3)	0·0 (7)	−0·2 (4)	−0·31 (9)	−0·12 (3)
	$U_{11}+U_{12}$†	6·4 (4)	5·2 (4)	6·9 (9)	6·2 (4)	6·68 (11)	6·56 (5)
	$U_{11}-U_{12}$†	7·2 (4)	5·8 (4)	6·9 (9)	6·6 (4)	7·30 (11)	6·80 (5)
	U_{33}	4·6 (5)	4·5 (3)	4·4 (5)	4·0 (2)	4·67 (4)	4·81 (7)
O	$x=y$	0·30478 (6)	0·30476 (6)	0·3048 (1)	0·30498 (11)	0·30493 (7)	0·30491 (5)
	U_{11}	5·2 (1)	5·7 (1)	5·4 (3)	5·0 (2)	6·01 (9)	5·31 (6)
	U_{12}	−2·0 (2)	−1·9 (1)	−2·0 (3)	−2·1 (1)	−3·72 (22)	−1·8 (1)
	$U_{11}+U_{12}$†	3·2 (2)	3·8 (1)	3·4 (4)	2·9 (2)	2·29 (24)	3·51 (12)
	$U_{11}-U_{12}$†	7·2 (2)	7·6 (1)	7·4 (4)	7·1 (2)	9·73 (24)	7·11 (12)
	U_{33}	3·5 (2)	4·4 (1)	4·1 (3)	3·6 (3)	4·54 (11)	4·0 (1)

* The thermal parameters in this column have been converted from β values.

† The entries $U_{11}+U_{12}$ and $U_{11}-U_{12}$ are the mean-square displacements along [110] and [1$\bar{1}$0] respectively, these being principal axes of the thermal vibration ellipsoids for (both) the atoms. The mean-square displacements along the third principal axis, [001], are given directly by U_{33}.

Table 4. *Atomic positional and anisotropic thermal parameters* ($Å^2 \times 10^3$) *for anatase at room temperature*

	Neutron determinations		Single-crystal X-ray determination
	Powder	Powder (TOF)	
	Present work	Burdett *et al.*	Horn *et al.*
Ti U_{11}	5·2 (3)	3·8 (2)*	4·9 (7)
U_{33}	7·0 (4)	3·8 (2)*	4·9 (4)
O z	0·20806 (5)	0·20814 (5)	0·2081 (2)
U_{11}	11·7 (4)	11·0 (3)†	9·2 (12)
U_{22}	2·7 (3)	4·3 (2)†	6·4 (12)
U_{33}	7·2 (3)	5·8 (1)	7·7 (11)

* Burdett *et al.* (1987) inadvertantly constrained the values of these two parameters to be equal.

† The values for U_{11} and U_{22} are shown reversed compared with the values tabulated by Burdett *et al.* (1987). This reversal is to convert the results to our particular setting and origin choice.

Burdett *et al.* analysis. It is concluded that for neutron powder diffraction data, obtained using either a conventional or TOF diffractometer, the Rietveld method provides reliable and realistic values for the structural and thermal parameters and their e.s.d.'s. We note in passing that the results from the earlier neutron powder diffraction study of rutile (Sabine & Howard, 1982) are (given the larger e.s.d.'s in that work) in satisfactory agreement with the results presented here.

For rutile, comparisons are possible of the results from neutron powder and neutron single-crystal investigations. The present powder results agree well with those obtained by Gonschorek & Feld (1982) from their single-crystal measurements, the maximum discrepancy being 1·2 combined e.s.d.'s. This is taken as further evidence that neutron powder diffraction, analysed by the Rietveld method, gives reliable results.

Comparisons of neutron with X-ray results are available for both compounds. The X-ray investigations referred to in the tables all make use of single crystals. The agreement of the present results for rutile with results from Abrahams & Bernstein (1971) is extremely good, the maximum discrepancy of 1·2 combined e.s.d.'s being for the positional parameter in this case. The agreement with the results from other X-ray studies of rutile is also satisfactory. For anatase, the differences between values of thermal vibration parameters obtained in the present neutron work and the X-ray work range up to three combined e.s.d.'s, making these differences comparable with differences between the neutron studies. The agreement between the values from neutron and X-ray refinements encourages confidence in all the results. The X-ray/neutron comparison allows comment on the polarization of the oxygen atom in rutile, as follows.

4.2. *The question of polarization of the oxygen atom in rutile*

The high static dielectric constant of rutile (Parker, 1961) has long been a matter for discussion (Traylor *et al.*, 1971; Gonschorek, 1982, and references cited therein). The oxygen polarizability is reportedly high (Tessman, Kahn & Shockley, 1953), and it has been suggested that the oxygen atom may indeed be highly polarized in rutile in its normal crystalline state. Suggested values for the dipole moment of the oxygen ion are about 0·8 e Å (Kingsbury, 1968; Bertaut, 1978), which would correspond to a displacement by about 0·1 Å of the electron cloud from the nucleus. As recognized by Bertaut, this would lead to a difference of about 0·015 between the value for the oxygen positional parameter determined by X-rays and that obtained in a neutron diffraction experiment. Such a difference would be readily detectable.

The X-ray study by Gonschorek (1982) and the neutron study by Gonschorek & Feld (1982) were carried out mainly to check whether there is a shift in the oxygen positional parameter between the X-ray and the neutron measurement. There was no significant difference between the oxygen positional parameters determined in the X-ray and neutron experiments (Table 3). In an independent study, Sabine & Howard (1982) determined the oxygen

positional parameter by Rietveld refinement from neutron powder diffraction data, and compared this result with those reported in the literature from X-ray single-crystal investigations. There was again no significant difference between X-ray and neutron-determined values for the oxygen positional parameter. Taking weighted means of the results recorded in Table 3, we now have $x_O = y_O = 0{\cdot}30492\ (4)$ from the X-ray measurements, and $x_O = y_O = 0{\cdot}30478\ (4)$ from neutron measurements. The difference between the mean results from the X-ray and neutron experiments referenced in Table 3 is 0·00014 (6) which is two orders of magnitude less than suggested by Kingsbury (1968) or Bertaut (1978).

4.3. *Comments on structure and vibrations in rutile and anatase*

The structures of rutile and anatase have been fully described in earlier work (*e.g.* Burdett *et al.*, 1987). Each structure can be seen as an assembly of linear O—Ti—O 'molecules' (Vegard, 1916), which are parallel to [110] and [1$\bar{1}$0] in rutile and to [001] in anatase. The length of the Ti—O bond in this 'molecule' (which is not the shortest Ti—O distance in either structure) is 1·98 Å at 295 K.

In rutile, we find (Table 3) that the thermal vibrations of the Ti atom are larger than the O-atom vibrations. In this respect, our results differ from those from the TOF study (Burdett *et al.*, 1987) which showed the Ti and O vibrations to be similar at 295 K. However, our results are in agreement with those from the single-crystal neutron work (Gonschorek & Feld, 1982) and the X-ray studies. The principal axes of the thermal vibration ellipsoids in rutile lie along [110], [$\bar{1}$10] and [001], the mean-square vibrational amplitudes in these directions being $U_{11} + U_{12}$, $U_{11} - U_{12}$ and U_{33}, respectively. The values of these quantities are included in Table 3. The largest vibrations of the Ti and O atoms are in the (001) planes, perpendicular to the 'molecule' described above, the O-atom vibrations being noticeably smaller in the other directions. We suggest that the anisotropy of the O vibrations is a reflection of the stereochemistry, since the separation in the [$\bar{1}$10] direction of the rows of molecules lying along [110] is $a/2^{1/2}$, which is a generous 3·25 Å. Thermal vibration anisotropies of a similar kind have been observed in neutron diffraction studies of SnO_2 and β-PbO_2 carried out in this laboratory, and such vibrational anisotropy may be a general feature in structures of the rutile type.

In the case of anatase, the heavier Ti atom vibrates less than the O atom. The vibration of the O atom is markedly anisotropic. Since its nearest neighbour in the x direction is another O at a distance a (3·785 Å), whereas there is another O—Ti—O 'molecule' at a distance $a/2^{1/2}$ (1·89 Å) in the y direction, we again associate the vibrational anisotropy with the stereochemistry. The greater degree of anisotropy in anatase (as compared with rutile) may relate to its more open crystal structure.

Table 5. *Debye temperatures* (K) *from diffraction data*

Measurement temperature	Rutile	Anatase
15 K	582 (10)	522 (10)
295 K	600 (10)	520 (10)

4.4. *The Debye temperature*

Ideally, it should be possible to compute the elements of the U matrix from the lattice dynamics of rutile and anatase, and to compare the computed values with those obtained in the diffraction studies and recorded in the tables above. However, the only thorough lattice-dynamical study is for rutile (Traylor *et al.*, 1971), and that provides information only at room temperature. The calculation is in any case beyond the scope of the present work.

A quicker but much less precise commentary can be made through the estimation of Debye temperatures. The solids are modelled as comprising atoms of the average mass undergoing isotropic vibrations of average amplitude. It is also assumed the frequency distribution can be approximated by the Debye model. In this approximation, a value for the Debye temperature determined by diffraction methods (Θ_M) can be calculated from the tabulated U values using the formulae given by Willis & Pryor (1975). The mass was taken to be the average for one Ti and two O atoms, and the mean-square displacement was taken to be the average of the diagonal elements of the U matrix for each atom averaged over the atoms. Debye temperatures were estimated from the room-temperature results from the present work and from the 15 K results reported by Burdett *et al.* (1987). The results are shown in Table 5. For rutile, the results for Θ_M may be compared with the Debye temperatures determined from specific heat measurements (Θ_C) by Sandin & Keesom (1969) and by Pandey (1965), which are also shown by Traylor *et al.* (1971). The room-temperature value for Θ_M is considerably lower than the corresponding value for Θ_C, which is 778 (5) K (Pandey, 1965). The values of Θ_M and Θ_C are not necessarily equal (Willis & Pryor, 1975), and a similar discrepancy has been reported in CaF_2 (Elcombe & Pryor, 1970).

We thank Mrs Joanne Warner for assistance with specimen preparation, and Dr Erich Kisi for making available to us his results on β-PbO_2.

References

ABRAHAMS, S. C. & BERNSTEIN, J. L. (1971). *J. Chem. Phys.* **55**, 3206–3211.
BERTAUT, E. F. (1978). *J. Phys. (Paris)*, **39**, 1331–1348.
BURDETT, J. K., HUGHBANKS, T., MILLER, G. J., RICHARDSON, J. W. & SMITH, J. V. (1987). *J. Am. Chem. Soc.* **109**, 3639–3646.
CAGLIOTI, G., PAOLETTI, A. & RICCI, F. P. (1958). *Nucl. Instrum.* **3**, 223–228.
CROMER, D. T. & HERRINGTON, K. (1955). *J. Am. Chem. Soc.* **77**, 4708–4709.
DOLLASE, W. A. (1986). *J. Appl. Cryst.* **19**, 267–272.
ELCOMBE, M. M. & PRYOR, A. W. (1970). *J. Phys. C*, **3**, 492–499.
GONSCHOREK, W. (1982). *Z. Kristallogr.* **160**, 187–203.
GONSCHOREK, W. & FELD, R. (1982). *Z. Kristallogr.* **161**, 1–5.
HILL, R. J. & HOWARD, C. J. (1986). Australian Atomic Energy Commission Report No. M112. AAEC (now ANSTO), Lucas Heights Research Laboratories, New South Wales, Australia.
HORN, M., SCHWERDTFEGER, C. F. & MEAGHER, E. P. (1972). *Z. Kristallogr.* **136**, 273–281.
HOWARD, C. J., BALL, C. J., DAVIS, R. L. & ELCOMBE, M. M. (1983). *Aust. J. Phys.* **36**, 507–518.
KINGSBURY, P. I. (1968). *Acta Cryst.* A**24**, 578–579.
MARCH, A. (1932). *Z. Kristallogr.* **81**, 285–297.
PANDEY, H. N. (1965). *Phys. Status Solidi*, **11**, 743–751.
PARKER, R. A. (1961). *Phys. Rev.* **124**, 1719–1722.
PETERSE, W. J. A. M. & PALM, J. H. (1966). *Acta Cryst.* **20**, 147–150.
RAO, K. V. K., NAIDU, S. V. N. & IYENGAR, L. (1970). *J. Am. Ceram. Soc.* **53**, 124–126.
RIETVELD, H. M. (1969). *J. Appl. Cryst.* **2**, 65–71.
SABINE, T. M. (1985). *Aust. J. Phys.* **38**, 507–518.
SABINE, T. M. (1988). *Acta Cryst.* A**44**, 368–373.
SABINE, T. M. & HOWARD, C. J. (1982). *Acta Cryst.* B**38**, 701–702.
SABINE, T. M., VON DREELE, R. B. & JORGENSEN, J.-E. (1988). *Acta Cryst.* A**44**, 374–379.
SANDIN, T. R. & KEESOM, P. H. (1969). *Phys. Rev.* **177**, 1370–1383.
SHINTANI, H., SATO, S. & SAITO, Y. (1975). *Acta Cryst.* B**31**, 1981–1982.
STRAUMANIS, M. E., EJIMA, T. & JAMES, W. J. (1961). *Acta Cryst.* **14**, 493–497.
TESSMAN, J. R., KAHN, A. H. & SHOCKLEY, W. (1953). *Phys. Rev.* **92**, 890–895.
TRAYLOR, J. G., SMITH, H. G., NICKLOW, R. M. & WILKINSON, M. K. (1971). *Phys. Rev. B*, **3**, 3457–3472.
VEGARD, L. (1916). *Philos. Mag.* **32**, 505–518.
WILLIS, B. T. M. & PRYOR, A. W. (1975). *Thermal Vibrations in Crystallography*, pp. 122–128. Cambridge Univ. Press.
YOUNG, R. A., PRINCE, E. & SPARKS, R. A. (1982). *J. Appl. Cryst.* **15**, 357–359.

Acta Cryst. (1991). B**47**, 468–473

Crystal Chemistry of Inorganic Phosphites

BY J. LOUB

Department of Inorganic Chemistry, Charles University, Hlavova 8/2030, 12840 *Praha* 2, *Czechoslovakia*

(*Received* 17 *April* 1990; *accepted* 21 *February* 1991)

Abstract

The results of X-ray structural analyses of inorganic phosphites are discussed and the average bond distances and angles of the HPO_3 group have been calculated by statistical evaluation of the geometry of the structures: P—O_s = 1·498 (16), P—O_m = 1·514 (12), P—O_l = 1·548 (22), H—P = 1·30 (8) Å, O_s—P—O_m = 114·0 (2·8), O_s—P—O_l = 110·7 (2·4), O_m—P—O_l = 109·8 (3·1), H—P—O_s = 109 (4), H—P—O_m = 107 (3) and H—P—O_l = 106 (5)° (the subscripts *s*, *m* and *l* indicate small, medium and large according to the P—O distances P—$O_s \leq$ P—$O_m \leq$ P—O_l). The bond-valence parameters $r_o(HP^{4+}—O^{2-})$ = 1·626 (5) and $r_o(H_2P^{3+}—O^{2-})$ = 1·642 (16) have been obtained. Correlations have been found between the P—O distance and the opposite O—P—O angle, and between the P—O distance and the $S(s)$ bond valence of the O(P) atom.

Introduction

The species $0{\cdot}5H^+$ and/or $0{\cdot}5H_2O$ can formally be gradually dissociated from phosphorous acid, H_3PO_3, yielding the phosphite types given in Table 1. Some of the phosphite types which are underlined in Table 1 and denoted by the letters *A* to *F*, have been found in solid phosphites (Loub & Kratochvíl, 1987). The present paper summarizes results of structure determinations of solid phosphites and phosphorous acid (see Table 2).* The phosphite structural types were systematized and attempts made to find some dependences among their properties so that certain results could be evaluated or predicted on this basis.

Structural types of phosphites

Substances characterized by a simple chemical formula may sometimes have very complicated structures. Therefore, the structures of some types are briefly characterized below.

Phosphites with a P:O *ratio of* 1:3

Phosphorous acid, H_3PO_3 (type *A*) (Fig. 1*a*), primarily belongs in this group. The acid molecules

* Lists of the full references used in Table 2 have been deposited with the British Library Document Supply Centre as Supplementary Publication No. SUP 54006 (5 pp.). Copies may be obtained through The Technical Editor, International Union of Crystallography, 5 Abbey Square, Chester CH1 2HU, England.

0108-7681/91/040468-06$03.00

© 1991 International Union of Crystallography